

## Structural transitions in DNA driven by external force and torque

Abhijit Sarkar,<sup>1</sup> Jean-Francois Léger,<sup>2</sup> Didier Chatenay,<sup>2</sup> and John F. Marko<sup>1</sup>

<sup>1</sup>*Department of Physics, The University of Illinois at Chicago, 845 West Taylor Street, Chicago, Illinois 60607*

<sup>2</sup>*LDFC, UMR CNRS 7506 and Université Louis Pasteur, Institute de Physique, 3 rue de l'Université, 67000 Strasbourg, France*

(Received 27 November 2000; published 12 April 2001)

Experiments on single DNA molecules have shown that abrupt transitions between states of different extensions can be driven by stretching and twisting. Here we show how a simple statistical-mechanical model can be used to globally fit experimental force-extension data of Léger *et al.* [Phys. Rev. Lett. **83**, 1066 (1999)], over a wide range of DNA molecule twisting. We obtain the mean twists, extensions, and free energies of the five DNA states found experimentally. We also predict global force-torque and force-linking number phase diagrams for DNA. At zero force, the unwinding torque for zero-force structural transition from the double helix to an unwound structure is found to be  $\approx -2k_B T$ , while the right-handed torque needed to drive DNA to a highly overwound state  $\approx 7k_B T$ .

DOI: 10.1103/PhysRevE.63.051903

PACS number(s): 87.14.Gg, 36.20.Ey, 64.90.+b

### I. INTRODUCTION

Development of micromanipulation techniques has allowed precise experiments to be done studying the mechanical properties of single molecules. One of the types of molecules which has been most intensely studied in this way is double-stranded (ds) DNA. When a dsDNA is not under appreciable stress, its two strands firmly hydrogen-bond together to form a right-handed double helix, with a helix repeat of about 3.5 nm, containing 10.5 base-pairs (bp). This classical ‘‘B-DNA’’ structure [1] is the basic DNA conformation found inside living cells. B-DNA is stable in physiological aqueous solution, i.e., water with buffered pH near 7.5, and with univalent salt of roughly 0.1 M concentration.

The hydrogen-bonding ‘‘base pairing’’ and hydrophobic ‘‘stacking’’ interactions which stabilize B-DNA involve free energies of only a few  $k_B T$  per base pair [2]. Therefore, when forces on the order of  $\approx 10k_B T/\text{nm}$  are applied to B-DNA, it will change conformation to some other DNA structure. At room temperature, a  $k_B T/\text{nm}$  is 4 piconewtons (pN), and so we should expect DNA structural transitions to be associated with forces on the order of 40 pN.

In fact, experiments by Cluzel *et al.* [3] and Smith *et al.* [4] showed that indeed a sharp structural transition occurs in dsDNA when under roughly 65 pN of tension. The experimental signature for this transition was a force ‘‘plateau’’ connecting B-DNA to a new DNA structure about 1.7 times the length of the double helix. This dramatic transition is possible due to the fact that the covalently bonded sugar-phosphate backbones along each strand are helically coiled inside B-DNA. Other DNA-stretching experiments have indicated that dsDNA can be stretched to as much as double its B-form length [5,6], close to full extension of the sugar-phosphate backbones. This new stretched DNA state is widely called ‘‘S-DNA’’ (against the wishes of one of the present authors who argued against a nomenclature forcing us to talk about the ‘‘B-S transition’’). In any case, this transition has been observed in many laboratories, and has in fact been used as a force calibration in a number of experiments.

Severe DNA conformational rearrangements are of basic biological interest, since DNA is routinely strongly deformed

during cellular processes. For example, many proteins deform DNA via stresses applied through their binding interactions. Some important examples are the transcription factor TBP which bends dsDNA through nearly a right angle over only a few base pairs [7], DNA-packaging histones which bend 146 bp of dsDNA through 1.75 circular turns [8], and the protein RecA which is capable of polymerizing along dsDNA so as to extend it to 1.5 times its B-DNA length [9,10]. It is perfectly reasonable that proteins can severely deform DNA, since the interactions responsible for binding of proteins to DNA are at the same energy scale (a few  $k_B T$  per contact) as those holding DNA into its B-form structure.

The 65 pN B-S transition described above occurs on dsDNAs with single-strand attachments at their ends, or on molecules with single-strand breaks (‘‘nicks’’) somewhere inside them. Such molecules cannot support torsional stress, and thus the 65 pN transition occurs under zero torque, or freely twisting conditions. In order for the molecule to extend to 1.7 times its B-form length, it seems likely that the two strands must untwist as well. However, most experiments on freely twisting molecules cannot address the question of the twist state of S-DNA, since they are done on molecules inside of which the twist can freely change.

In order to study the twisting of S-DNA it is necessary to torsionally constrain and twist dsDNAs. Two groups have developed experimental techniques to do this, that of Strick *et al.* [11] and Cluzel *et al.* [12,13]. These experiments allow one to measure the force-extension curve for a dsDNA subject to the constraint that its double-helix linking number (essentially the number of times that the two strands are wrapped about the other) is fixed. Early experiments by Strick *et al.* [11] showed that for low forces  $< 5$  pN, effects on the entropic elasticity of DNA could be observed and studied, as a function of twisting. Studies of this low-force regime verified theoretical predictions of coexistence of supercoiled and extended domains [14], and denaturation of undertwisted DNA at forces of a few pN. Subsequent and detailed theoretical studies [15–17] have painted a rather complete picture of the low-force behavior of twisted DNA.

Slightly later experiments by the same group explored the

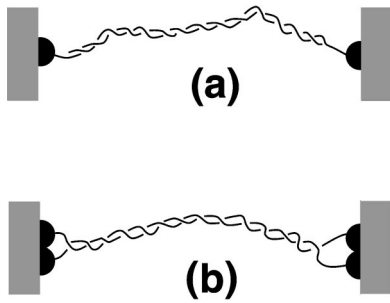


FIG. 1. Schematic of different attachment schemes for a single molecule of double-stranded DNA (coils) to the force transducer (bulges). (a) Shows single strand attachment which allows Lk to fluctuate freely. (b) Illustrates topology-fixing double strand attachment.

behavior of twisted DNA at higher forces, and showed that dsDNA could be denatured by untwisting [18,19], and very heavily overtwisted [20]. Finally, work of Leger *et al.* [13] made a global study of the force-extension behavior over a wide range of twisting, and for large forces in the range 1–100 pN. Remarkably, those experiments found four force-plateau-type transitions, suggesting that four DNA states in addition to B-DNA can be accessed using different forces and twisting. However, a full interpretation of the experimental results requires a theoretical analysis.

In this paper, we construct a simple statistical mechanical model of mechanically stressed double stranded DNA with its twist fixed externally and exactly evaluate its partition function by numerically diagonalizing the transfer matrix. We determine the parameters of our model by a fit of the theoretical force-extension curves to those of experiment [13]. The plan of the paper is as follows. In Sec. II we discuss the experimental results and the DNA structures that have been proposed to explain them. In Sec. III we present our model, which is essentially a discretized version of the model discussed in a previous short communication [13]. In Sec. IV, we show the results of the theory in comparison with experiment, and we discuss its implications.

## II. EXPERIMENTAL DATA ON DNA OVERSTRETCHING

### A. Freely untwisting molecule

In micromanipulation experiments, DNA linkage will be free to change if single-strand attachments are made to the molecule [Fig. 1(a)], or if there is a break (a “nick”) in either of the two sugar-phosphate backbones. The elastic response of nicked DNA has four regimes [Fig. 2(a)]: first, thermal bending fluctuations are removed by application of small forces ( $<10$  pN). By 10 pN the molecule is completely extended to its full B-form contour length,  $\approx 15 \mu\text{m}$  for  $\lambda$ -DNA [21–25]. The force needed to stretch the molecule further rises linearly with extension up to  $\approx 65$  pN, and a linear stretching elastic constant can be roughly estimated from the slope ( $220k_B T/\text{nm} = 900$  pN). Then, at 65 pN, the molecule extends abruptly over a narrow range of force ( $\approx 5$  pN), from about 1.1 times to about 1.7 times its unstressed B-form contour length [3,4]. The linear relationship

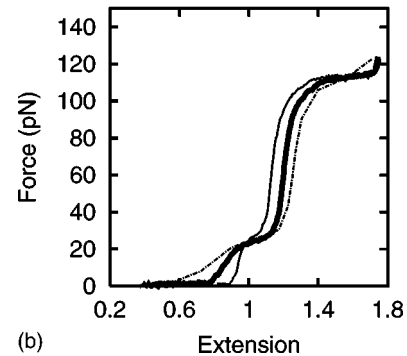
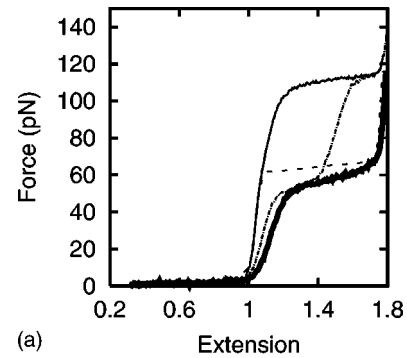


FIG. 2. Force versus extension for DNA with different fixed negative and positive  $\sigma$ . (a) Shows data for nicked DNA (dashed),  $\sigma=0.00$  (solid thin),  $-0.357$  (dot-dashed), and  $-0.714$  (solid thick). Note that  $\sigma=-0.714$  curve coincides with the nicked DNA curve at the end of the 65 pN plateau. This is used to extract the helicity of S-DNA. (b) Shows the elastic response of overwound DNA with  $\sigma=0.357$  (solid thin),  $0.714$  (solid thick), and  $1.071$  (dot dashed).

between force and extension resumes after the transition but with a larger elastic constant [3,4].

The behavior at  $\approx 65$  pN has been interpreted as a cooperative transition from one well-defined structural state of DNA (B-form DNA at low forces) to another (S-form DNA at high forces) [3]. The precise structure of S-DNA is unknown. Although a ladderlike form has been proposed [4,26], S-DNA is less than the 2 times B-form length expected for complete unwinding of the double helix. In comparison with experiments on isolated single-stranded DNA, S-DNA is seen to have a different force-extension behavior [4], indicating that the two strands of an S-DNA are strongly interacting.

### B. Fixed linking number

For dsDNA with both strands affixed to surfaces [Fig. 1(b)], the linking number Lk of the two strands is a topological invariant. Lk is the sum of the twist (Tw, the number of times one sugar-phosphate backbone wraps around the other) and the writhe (Wr, the average over all projections of the number of nonlocal self-crossings of the double helix) [29,30]:

$$\text{Lk} = \text{Tw} + \text{Wr}. \quad (1)$$

Experiments which fix DNA topology are usually done with

initially relaxed molecules, with  $Wr$  near 0. For a long straight and unstressed DNA,  $Lk=Lk_0$ , the number of turns of the double helix. Since there is one turn every 10.5 bp for unstressed DNA,  $Lk_0 \approx N_{bp}/10.5$ , where  $N_{bp}$  is the total number of base pairs. This implies for  $\lambda$ -DNA a  $Lk_0$  of  $\approx 4200$ . It is convenient to describe the linkage by the fractions of turns added or removed:

$$\sigma = \frac{Lk - Lk_0}{Lk_0}. \quad (2)$$

For either a ladderlike DNA structure, or for separated single strands,  $\sigma = -1$ . By comparison, DNA *in vivo* is usually constrained to have  $\sigma \approx -0.05$ .

Figure 2(a) shows the force-extension response of torsionally constrained DNA with  $\sigma=0$ , i.e.,  $Lk = Lk_0$ . A force plateau is observed at 110 pN, nearly double the force of the B-S transition on a nicked molecule. The transition with  $\sigma=0$  is also somewhat more gradual and ‘‘rounded’’ than the nicked molecule transition. These data already make clear that S-DNA is not simply denatured DNA, and that the fixed linkage constraint introduces another DNA state characterized by a higher free energy.

For  $\sigma < 0$ , a new force plateau appears in Fig. 2(a) at  $\approx 50$  pN. As the molecule is progressively underwound (as  $\sigma$  is made more negative) the width of the lower 50 pN plateau increases at the expense of the upper 110 pN transition. The 110 pN transition completely disappears at  $\sigma \approx -0.7$ . The  $\sigma = -0.714$  curve coincides with the nicked DNA curve at the end of the 65 pN plateau. This indicates that ‘‘pure’’ S-DNA has  $\sigma \approx -0.7$ . A progressive softening of the DNA with underwinding is also apparent in the data [13].

Our explanation of the  $\sigma=0$  transition is that the linking number constraint obstructs the production of ‘‘pure’’ S-DNA at 65 pN. Instead, a mixture of two phases, S-form and some other form of dsDNA, must arise to satisfy the twist constraint. Work of the group of Allemand *et al.* [20] has shown that dsDNA can organize into a highly overtwisted ‘P’-form with a 2.4 bp helix repeat, or  $\sigma = +3.375$ . It is possible that P-DNA is created along with S in suitable proportion to produce the necessary total linking number, and that the 110 pN force is characteristic of the transition to the P-state. Given the twist of P measured by Allemand *et al.* and the S-DNA twist of  $\sigma \approx -0.7$ , for  $\sigma=0$  this mixture should be about 4/5 S to 1/5 P. This is in accord with the observed overextension of 1.66 times the native  $\lambda$ -DNA length at 110 pN for  $\sigma=0$ , the appropriately weighed average of S- and P-form extensions [13].

The appearance of the second transition plateau at  $\approx 50$  pN and the progressive narrowing of the 110 pN plateau for  $\sigma < 0$  can be fit into this picture as follows. Initially, unwinding is stored in an untwisted double helix. Once a force of  $\approx 50$  pN is applied, the untwisted part of the molecule transforms to S-form and the remainder of the molecule is still B-DNA with  $\sigma=0$  and will display a transition at  $\approx 110$  pN. Further unwinding narrows the 110 pN plateau while widening the one at 50 pN since a progressively larger fraction of the molecule can transform to S-DNA at 50 pN. This picture of the  $\sigma < 0$  transitions means that the  $\sigma$  for which the 110

pN completely disappears for the first time is a direct measurement of the helicity of S-DNA. This happens at  $\sigma = -0.714$ , implying a S-DNA helix pitch of 22 nm and 37.5 base pairs per turn.

Figure 2(b) shows data for force-extension response of overwound DNA for  $\sigma = +0.357, +0.714, +1.071$  [13]. A new force plateau near 25 pN occurs, which was first reported by Allemand *et al.* [20]. With increasing  $\sigma$ , the 25 pN transition widens while the 110 pN transition narrows. For higher  $\sigma$ 's, the molecule stretching modulus shows considerable softening for forces  $< 20$  pN.

The 25 pN transition for overwound DNA is thought to be a straightening of plectonemically supercoiled P-DNA [13,20]. Overwinding the molecule from  $\sigma=0$  to  $\sigma=1.071$ , the molecule fraction which must transform to unwritten P-DNA increases, widening the 25 pN plateau (from initially zero width) while narrowing the 110 pN plateau.

The  $\sigma$  for which the 110 pN transition completely disappears corresponds to the point where the entire molecule is able to transform to P-DNA at the 25 pN transition. In this way, Leger *et al.* measured P-DNA to have a helix repeat of  $\approx 2.62$  bp/turn and an extension of 1.6 times the B-form length [13]. This is close to the 2.4 bp/turn and the 1.75 extension estimates of Allemand *et al.* [20].

The interpretation of the fixed  $\sigma$  experiments raises a number of questions. For  $\sigma < 0$  and forces less than 50 pN, is the molecule initially in a pure B-DNA structure, or is it coexisting with some other structure so that there can be *two* reasonably sharp transitions as force is increased? If B-DNA does coexist with some other structure below 50 pN, what does this structure look like? Since the 50 pN plateau is seen only for  $\sigma < 0$  and not for  $\sigma=0$ , we conclude that this phase must have nonzero helicity. From inspection of the experimental data we also expect the phase to have a contour length similar to B-DNA.

### III. MODEL

We have constructed a simple one-dimensional (1D) statistical mechanical lattice model of DNA to test the proposed transition mechanisms and to explore in detail questions such as those raised in the previous paragraph. Our model is a generalization of a previous model proposed in Cluzel *et al.* [3] to explain the B-form to S-form transition. We modify it to take into account the fixed twist constraint and the local harmonic fluctuations of twist density and extension about their equilibrium values. This model is also a discretized version of a continuum model presented in Ref. [13] to explain the fixed twist experiments. Our discrete model leads to much faster numerical calculations and lets us explore the phase diagram of DNA more thoroughly.

As might be expected, there are quite large differences in the force-driven structural transitions displayed by synthetic pure AT and pure GC molecules [6]. Sequence effects can in principle be added to our calculations, but the available data are far from adequate to fix the many parameters required. Given this state of affairs, plus the observation of little change of the B-S transition when different natural-sequence



molecules are used [10], we consider a homogeneous model in this paper.

### A. Definition of the model

To understand the complicated plateau curves of Fig. 2 and their evolution with  $\sigma$ , we treat them as being due to transitions between five microscopically distinct structural states. Which states participate in a transition depends on  $\sigma$ . The micromanipulation experiments control only extension and linkage number, and therefore our model specifies only the microscopic extensions and linkage numbers of the five states. Further details of the secondary structures of the various DNA states cannot be directly inferred from the available experimental data, and therefore we do not attempt to predict them.

The five states that we consider include B-DNA which is stable at zero force and zero torque, and the overstretched S- and P-DNA states, which are underwound and overwound, respectively. This leaves two more states, which we have found to be essential in producing the two-plateau force-distance curves found in the intermediate  $\sigma$  parts of Fig. 2. To fit the data, one of these states must be highly overwound and highly contracted, implying the supercoiled P state (sc-P-DNA) proposed by Allemand *et al.* [20]. The final state must be more underwound than the S-state, but extended to a length comparable to B-DNA. Since our fitting suggests a left-handed double helix, we call this state ‘‘Z’’-DNA in analogy with an actual left-handed double helix structure observed for certain sequences and chemical conditions [27].

DNA is modeled as a 1D lattice with each lattice site degree of freedom  $n_i$  (with the subscript  $i$  labeling the lattice sites) having one of five possible integer values from 0 to 4 representing 5 different microscopic structures (0: B-DNA, 1: S-DNA, 2: P-DNA, 3: ‘‘Z’’-DNA and 4: sc-P-DNA).

Each structure has a characteristic dimensionless linkage number density  $\bar{\theta}_n$  which measures the excess linkage density in radians per base pair of one of the DNA structural states relative to B-form DNA, and extension  $\bar{s}_n$  (fractional change in contour length relative to B-DNA) about which we allow harmonic fluctuations. The free energy cost relative to B-form DNA associated with creation of the stressed DNA states is taken into account with five more parameters  $\epsilon_n$ . By definition,  $\bar{\theta}_0=0$ ,  $\bar{s}_0=0$ , and  $\epsilon_0=0$ .

The Hamiltonian for our model is

$$\frac{H([n_i])}{k_B T} = \sum_i \frac{C'}{2} (\theta_{n_i} - \bar{\theta}_{n_i})^2 + \frac{K'}{2} (s_{n_i} - \bar{s}_{n_i})^2 + J(1 - \delta_{n_i, n_{i+1}}) + \epsilon_{n_i} - f \bar{s}_{n_i} - \tau \bar{\theta}_{n_i}. \quad (3)$$

$C'$  in our Hamiltonian is the usual twist persistence length  $C$  (between 75 to 110 nm; see below) divided by 0.34 nm to give a dimensionless harmonic twist fluctuation energy. Similarly,  $K'$  is the extensional elastic constant  $K$  ( $= 300 \text{ nm}^{-1}$ ; see below) times 0.34 nm. The force  $f$  and torque  $\tau$  are similarly reduced by factors of  $k_B T$  and 0.34 nm so as to be dimensionless.

The quadratic terms in  $\theta_n$  and  $s_n$  simply account for small deviations of linkage density and extension from their usual values  $\bar{\theta}_n$  and  $\bar{s}_n$ . The ‘‘domain wall’’ term  $J(1 - \delta_{n_i, n_{i+1}})$  states the molecule’s preference for structural uniformity, or equivalently the cooperativity of the various structural transitions. The force and torque couplings transmit the externally imposed stresses to the molecule.

At zero force and torque, the parameters of the model should be chosen so that state 0, B-DNA, is the lowest-energy state. The basic idea of the model is that for sufficiently large forces or torques, the other states can become lower in energy, causing first-order-like structural transitions. Of course a one-dimensional model will not produce truly discontinuous transitions, but instead will produce smoothed transitions similar to those observed experimentally (Fig. 2).

Our model does not include low force ( $< 4$  pN) entropic elasticity of DNA, which is not important at the high forces we are considering. The ‘‘softening’’ of the DNA extensional modulus in the linear regime  $< 50$  pN for  $\sigma < 0$  is also not captured by this model. These effects will be further discussed in the Conclusion.

### B. Transfer matrix calculation

We begin by integrating out the local harmonic fluctuations in  $\theta_n$  and  $s_n$ . This leads to additive contributions to the free energy and  $\langle \theta \rangle$  and  $\langle s \rangle$  are

$$\langle \theta_{n_i} \rangle = \bar{\theta}_{n_i} + \frac{\tau}{C'}, \quad (4)$$

$$\langle s_{n_i} \rangle = \bar{s}_{n_i} + \frac{f}{K'}. \quad (5)$$

Calculation of the partition function is now reduced to a transfer matrix diagonalization problem by rewriting it as

$$Z = \sum_{\{n_1\}, \dots, \{n_N\}} \prod_i T(n_i, n_{i+1}), \quad (6)$$

where

$$T(n_i, n_{i+1}) = \exp\{-\beta H_{\text{symm}}(n_i, n_{i+1})\}. \quad (7)$$

$H_{\text{symm}}$  is the symmetric nearest-neighbor Hamiltonian.

For a one-dimensional system with site-independent couplings and periodic boundary condition on the transfer matrix [ $T(n_N, n_{N+1}) = T(n_N, n_1) = T(n_1, n_N)$ ], Eq. (6) becomes

$$Z = \text{Tr}(T^N) = \sum_n \lambda_n^N, \quad (8)$$

where the  $\lambda_n$ ’s are the eigenvalues of the transfer matrix. The free energy  $F = -\beta^{-1} \ln[\sum_n (\lambda_n)^N]$ . In the thermodynamic limit, only the largest eigenvalue  $\lambda_{\text{max}}$  contributes to the sum so we have

$$F = -N\beta^{-1} \ln(\lambda_{\text{max}}). \quad (9)$$

The choice of boundary condition does not affect this result.

For our model, the transfer matrix is independent of which pairs of neighboring lattice sites we look at since we have homogeneous couplings. Also, the elastic fluctuations in  $s_{n_i}$  and  $\theta_{n_i}$  have been integrated out so they do not enter the model's transfer matrix. The transfer matrix is given by

$$T(n_i, n_{i+1}) = \exp \left[ J(\delta_{n_i, n_{i+1}} - 1) - \frac{1}{2}(\epsilon_{n_i} + \epsilon_{n_{i+1}}) + \frac{f}{2}(\bar{s}_{n_i} + \bar{s}_{n_{i+1}}) + \frac{\tau}{2}(\bar{\theta}_{n_i} + \bar{\theta}_{n_{i+1}}) \right]. \quad (10)$$

The average value of an operator dependent on adjacent sites  $\langle O \rangle$  can also be calculated by this method:

$$\langle O \rangle = \frac{\text{Tr}(SOS^{-1}T_d^N)}{Z}, \quad (11)$$

where  $T_d$  is the diagonalized transfer matrix and where  $S$  is the diagonalizing matrix. Two-point correlation functions can be similarly calculated using

$$\langle O_i O_{i+L} \rangle = \frac{\text{Tr}(SO_i S^{-1} T_d^L S O_{i+L} S^{-1} T_d^{N-L})}{Z} - \langle O_i \rangle \langle O_{i+L} \rangle. \quad (12)$$

The model is solved exactly by numerically diagonalizing the transfer matrix. This allows us to compute directly statistical averages for given values of force and torque. However, to contact the experimental results of Fig. 1 we also need to compute the torque necessary to make  $\langle \sigma \rangle = \sigma_{\text{ext}}$ . This must be done for each force and  $\sigma_{\text{ext}}$  of interest.

### C. Choice of values of fitting parameters

In all eighteen parameters need to be specified in our Hamiltonian to obtain the theoretical force-extension curves. These are  $C'$  (or  $C$ ),  $K'$  (or  $K$ ),  $J$ ,  $\epsilon_n$ ,  $\bar{\theta}_n$ , and  $\bar{s}_n$ , with  $n$  going from 0 to 4. However, many of these parameters are determined by previous experiments.

The stretch modulus  $K$  is known to be roughly  $300 \text{ nm}^{-1}$  [31,32], giving  $K' = 102$ .  $C$  is thought to be between 75 and 100 nm. Moroz and Nelson [15] have fit experimental data to obtain  $C = 110 \text{ nm}$ , while Bouchiat and Mezard find  $C \approx 70 \text{ nm}$  [16] and a value  $C = 75 \text{ nm}$  has been determined from studies of linkage number fluctuations in circular DNAs [33]. We use a  $C'$  of 220 which corresponds to  $C = 75 \text{ nm}$ . Finally, the parameters for the B-DNA state are defined as  $\bar{s}_0 = 0$ ,  $\bar{\theta}_0 = 0$ , and  $\epsilon_0 = 0$ .

S-DNA is known to be 1.7 times longer than B-DNA [3] and from Leger *et al.* [13], it is known to have a helicity (relative to B-DNA) of  $-1.33 \text{ nm}^{-1}$  (37.5 base pairs per turn). This fixes  $\bar{s}_1 = 0.7$  and  $\bar{\theta}_1 = -0.45$ . Next, we use the free-twist experimental data to fix the S-DNA free energy at  $\epsilon_1 = 3.7$  and the transition cooperativity at  $J = 2.0$ , in precisely the manner used by Cluzel *et al.* in their model of the B-S transition [3].

The P-DNA state was previously studied by two groups [20,13], and we take values for the stretch and linkage number which are between the values obtained in those experiments,  $\bar{s}_2 = 0.6$  and  $\bar{\theta}_2 = 1.87$ . Since the two experiments agree to about 10% on these two parameters, we are highly constrained as to their choice.

The parameters for the related sc-P-DNA state are also essentially determined by experiment [20,13]. Since supercoiled P-DNA will form plectonemic coils, its length will be essentially zero, i.e.,  $\bar{s}_4 = -1$ ; on the other hand its linkage number will be close to that of P; we take  $\bar{\theta}_4 = 1.87$ .

Finally, we have the ‘‘Z’’-DNA state, which from the experimental data is qualitatively understood to not be highly extended, and to be underwound. The ‘‘Z’’ stretch and linkage parameters must be determined by fitting of our model to experiment, and we determine  $\bar{s}_3 = 0.13$  and  $\bar{\theta}_3 = -1.30$ . Overall, the structural parameters for the five states are compatible to those used previously [13].

The parameters which are truly free for fitting are the free energies of the P, sc-P, and ‘‘Z’’ states. These are determined essentially by the plateau forces for the fixed- $\sigma$  transitions. We find  $\epsilon_3 = 2.3$  (‘‘Z’’),  $\epsilon_2 = 17.0$  (P), and  $\epsilon_4 = 13.5$  (sc-P). For S-, P-, and ‘‘Z’’-DNA the free energies are similar (to within 30% in the worst case) to the corresponding parameters in our previous work [13]. In the present paper the free energy of sc-P-DNA differs substantially from what was used in Leger *et al.*, being quite close to the free energy of P-DNA. The different free energy parameters found here are a consequence of differences between the two models, our earlier one being a continuum model vs the present one being discrete. In our earlier work there were additional free parameters for twist and stretch stiffnesses of each state, which make varying contributions to the free energies of the five states. In our present work, all states have the same stretch and twist stiffness, which make the relative free energies more closely related to the free energies of the five states.

## IV. RESULTS AND DISCUSSION

### A. DNA with unconstrained linking number

When we allow DNA linking number to fluctuate freely with zero applied torque, our model reproduces the usual B-form to S-form transition seen in experiments on nicked or single-strand-attached molecules. Figure 3(a) superposes the experimental data on our calculated force-extension curve. The length fraction  $\langle \delta_{n_i, m} \rangle$  of each of the states ( $m = 0, 1, 2, 3, 4$ ) is shown adjacent to the force extension curve as a function of force. Near 65 pN, we see B-DNA give way to S-DNA, resulting in a pure phase of S-DNA after  $\approx 70 \text{ pN}$ . The length fractions of the other phase are extremely close to zero due to their much higher free energies.

### B. DNA with fixed $\sigma \leq 0$

Figure 3(b) shows the theoretical force response curve superposed on the experimental data, for linking number  $\sigma = 0$ . Initially, the molecule starts off in pure B-form. Near 65

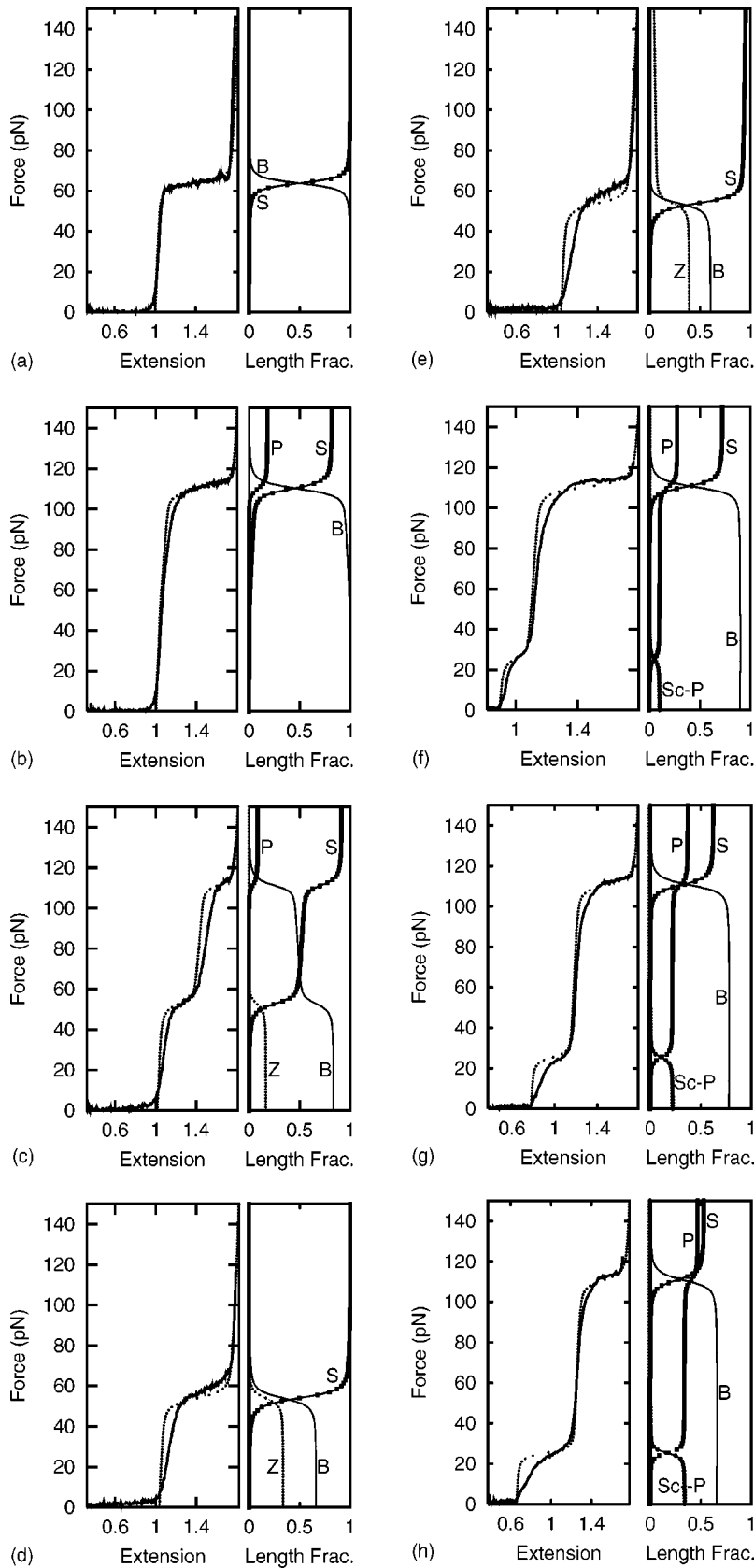


FIG. 3. Experimental force versus extension data for positive and negative  $\sigma$  and nicked DNA superposed on the corresponding theory curves together with the plots of force versus length fraction ( $\langle \delta_{n_i, m} \rangle$ ) for fixed  $\sigma$ . In all force-extension curves, the solid black line is the experimental data and the solid dot curve the theoretical fits. (a) shows computed (solid dots) and experimentally determined (solid black) force-extension data for nicked DNA. The adjacent B and S length fractions intersect at the transition force. Other phases are absent. (b)–(e) correspond to  $\sigma = 0.00, -0.357, -0.714,$  and  $-0.833,$  respectively. (f)–(h) correspond to  $\sigma = 0.357, 0.714, 1.071.$  In all these plots,  $\langle \delta_{n_i, m} \rangle$  is adjacent to the force-extension data. The fixed-topology constraint determines which structural states participate in the transition(s) for given  $\sigma$ . In all the plots, length fraction for B-DNA is shown by the solid line, for P by successive squares, for S by alternating solid squares and dashes, for “Z”-DNA by the solid dot curve, and for Sc-P by alternating solid dots separated by lines.

pN, an appreciable amount of S-DNA cannot form as in the unconstrained- $\sigma$  case since this would either violate the twist constraint (S-DNA is undertwisted), or cost a large amount of twist energy. Thus only a small density of S-DNA

“bubbles” form as force is raised from 65 to 110 pN. At 110 pN, the force is large enough for the molecule to transform from B into a mixture of S-form and P-form DNA. Since P-form DNA is overtwisted, it can compensate for the cre-

ation of the undertwisted S-DNA. This is evident in the roughly 4:1 proportionality of the length fractions for S- and P-DNA for forces  $> 100$  pN, which matches the proportionality of the S and P twisting.

The computed force-extension curves for underwound DNA for  $\sigma = -0.357$ ,  $-0.714$ , and  $-0.833$  are shown in Figs. 3(c), 3(d), and 3(e), respectively, along with experimental data. For  $\sigma = -0.357$  two transitions occur, one at  $\approx 50$  pN, followed by a second at  $\approx 110$  pN. The existence of two transitions requires the undertwisted ‘‘Z’’-DNA state to absorb the underwindings at low force. Without the ‘‘Z’’-state, we have found that S-DNA always appears immediately at low forces (without ‘‘Z’’, S would be the only underwound state in the model). Then, there could be one transition, corresponding to replacement of the B fraction with P. An additional problem in this case is that the zero-force state has an extension which is too long to fit the experimental data; note that this is a consequence of the zero-torque results which fix the S-DNA structural parameters.

Instead, we have a mixture of ‘‘Z-’’ and B-DNA at zero force in appropriate fractions to fix the net linking number at  $\sigma = -0.357$ . At  $\approx 50$  pN, the ‘‘Z’’-DNA portion and some of the B-DNA portion of the molecule transform to S form, giving a B-S mixture for forces between 50 and 100 pN. The width of this first transition is determined by the relative fractions of B and S necessitated by the underwinding. The exchange of S-DNA for ‘‘Z’’-DNA is seen clearly in the computed length fractions for these phases.

At 110 pN, the B-DNA portion is converted to a mixture of P- and S form DNA, in the same way as occurs in the  $\sigma = 0$  case. At larger forces, the molecule is thus predominantly in S form, with a small fraction of P-DNA as required to satisfy the linkage number constraint. At  $\sigma = -0.357$ , we start at low forces with ‘‘Z’’+B, and then in two steps we go to B+S and then to S+P. Without the ‘‘Z’’ state to start with, there would be no possibility for this sequence of two transitions.

As  $\sigma$  is reduced further, the fraction of the molecule in the ‘‘Z’’-DNA phase at low force progressively increases, and the fraction of the molecule which ends up as S-DNA after the 50 pN transition correspondingly increases. Thus, less and less B-DNA remains to participate in the 110 pN transition, and it becomes progressively narrower. Finally, for  $\sigma = -0.714$ , the 110 pN transition completely disappears indicating conversion of all the B+‘‘Z’’ DNA below 50 pN to ‘‘pure’’ S-DNA at 50 pN [Fig. 3(d)].

For even more underwinding [Fig. 3(e)], a large amount of ‘‘Z’’-DNA must initially be created. Then, in order to satisfy the twist constraint an appreciable fraction of ‘‘Z’’ survives at high forces. This occurs because the ‘‘Z’’ state is more underwound than is S.

A few discrepancies between theoretical and experimental curves are evident. The experimental data show a marked reduction in the low-force extensional modulus with underwinding. This effect is not in our model since we have only one stretch constant parameter for all five states; additional parameters might be able to take this effect into account. This difference in modulus causes the theoretical extension widths of the 50 pN B+‘‘Z’’ $\rightarrow$ B+S transitions to be wider

than those observed experimentally. Most likely, these differences are due to our oversimplification of the ‘‘Z’’ state, which is clearly appreciably softer in both twist and stretch than the other DNA states. Finally, we have ignored low force ( $< 10$  pN) entropic elasticity of B-DNA; our model of course does not reproduce the low force elastic regime where partially extended and plectonemically supercoiled B-DNA are found.

### C. DNA with $\sigma > 0$

Figures 3(f)–3(h) show the computed elastic response of DNA for the overwound cases  $\sigma = +0.357$ ,  $+0.714$ , and  $+1.071$ , overlaid on the experimental data. At zero force, the extra twists are absorbed in a collapsed supercoiled state sc-P-DNA [20]. This leads to coexistence of B- with sc-P-DNA at low forces. The experimental signature of this supercoiled state is the length reduction well below the B-form length. Near 25 pN, the supercoiled P-DNA extends to become P-DNA, giving the first transition. This is exactly analogous to similar transitions between plectonemically supercoiled B-DNA and extended B-DNA observed at forces  $\approx 1$  pN, although without the added complexity of appreciable conformational fluctuations [11,14].

Through this first 25 pN transition the B-DNA fraction is almost unchanged. Then, the B region undergoes the 110 pN transition to a mixture of S- and P-DNA with the proportion of DNA participating in these two states as is required by  $\sigma$ . The larger the number of extra twists inserted into the molecule, greater the proportion of DNA that is in sc-P form at zero force, and the greater the proportion of P-DNA at high force. Similarly, the extension width of the 25 pN transition broadens at the expense of the 110 pN transition as  $\sigma$  increases.

Again not all of the features of the transitions are captured by our simple model. As for  $\sigma < 0$ , the stretching modulus of the low-force (B+sc-P) drops as the molecule is overwound progressively more. This is not so surprising since the P form is known to have its base-pairing disrupted (see the Conclusion). Overall, the two-stage transitions are well described by our simple five-state model over a wide range of linkage number and force.

### D. Global phase diagram of DNA under stress

The preceding sections propose a simple model which semiquantitatively describes the structural transitions of a DNA driven by forces and torques. In fact, the transitions are experimentally sharp enough that it makes sense to talk about a ‘‘phase diagram.’’ This is most simply defined in terms of pure ‘‘phases’’ which are stable in different regions of the force-torque plane. We do not consider the modification of this phase diagram by changes in other parameters, e.g., temperature, pH, salt concentration, etc.

The thick lines of Fig. 4(a) show the boundaries between the five pure states as a function of force and torque. The lines themselves indicate the locus of points in the force-torque plane where there is no state which occurs with greater than 90% probability, indicating that the transitions are all rather sharp and first-order-like, with a typical width



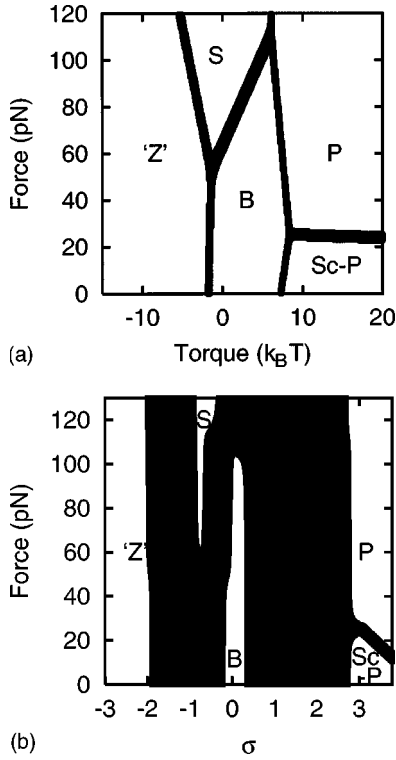


FIG. 4. The force-torque (a) and force- $\sigma$  (b) phase diagrams. In (a), regions separated by the diffuse border “lines” correspond to force-torque pairs for which the equilibrium DNA state is a pure structural phase. Inside the boundaries, adjacent phases coexist. Intersection of three phase boundary lines corresponds to a region of three phase coexistence—a “triple point.” In (b), the phase boundary lines of (a) are now greatly thickened leaving only slivers of pure S-form and B-form phases. The force- $\sigma$  pairs which fall inside the phase-boundaries correspond to DNA structural states with coexistence of adjacent pure phases.

of  $1 k_B T$  in torque, and 4 pN in force. The five phases also involve three triple-point-like regions where three phases can coexist.

For zero force and zero torque, we have B-DNA; then for  $f < 10$  pN, a transition to “Z”-DNA occurs for unwinding torque  $\approx -2k_B T$ , and a transition to sc-P occurs for overwinding with  $\approx +7k_B T$  of torque. These estimates are in very good agreement with the results of the independent prior analysis performed by Strick *et al.* [34] on force-extension data for fixed-twist molecules.

For forces  $> 20$  pN, sc-P DNA is replaced by P-DNA; the transition force between these two phases is essentially independent of torque since the P and sc-P states are nearly the same, except for having very different extensions. At a force  $\approx 50$  pN, S-DNA appears for the first time, for unwinding torques  $\approx -3k_B T$ . S-DNA remains stable at zero torque up to the highest forces that can be studied by micromanipulation, in agreement with experiments at zero torque which show only one transition, corresponding to B-S in our model.

Since all the transitions are relatively sharp, the state which is stable for given force and torque corresponds to that with lowest energy  $\Delta E_{n_i} = \epsilon_{n_i} - f\bar{s}_{n_i} - \tau\bar{\theta}_{n_i}$ . The results of the “zero-temperature” free energy minimization shows the

same phase diagram topology as in the thermal phase diagram with zero temperature phase boundaries overlapping with the exact phase boundaries, from which we conclude that the true force-torque phase diagram essentially corresponds to this “zero-temperature” estimate. Since force and torque appear linearly in the energy, the phase boundaries appear as a network of nearly straight line segments.

Figure 4(b) gives a phase diagram in the force-linking number ensemble. Since  $\sigma$  is a conserved quantity, it displays phase separation, so we have a phase diagram with coexistence regions (solid black) between the pure states (open regions). The three triple points of Fig. 4(a) have turned into “regions” with a continuum of forces and  $\sigma$ ’s for which the DNA is structurally in three pure phase coexistence. Finally, in each phase diagram, the boundaries between pure phases correspond to force- $\tau$  or force- $\sigma$  pairs for which the length fraction contributed by each of the five pure phases is less than 90%.

## V. CONCLUSION

### A. Five structural states occur in the DNA force-torque “phase diagram”

Our main result follows from experimental data [13], which show four distinct force “plateaus” which we take as the signatures of cooperative structural transitions to four non-B-DNA states. Although we have no direct microscopic information about these four new DNA states, the stretching-twisting experiments do allow determination of their mean extensions and linking numbers. For positive (right-handed) twisting, we find that one new state is extended and highly overtwisted (P-DNA), and another is its plectonemically supercoiled version (sc-P-DNA), which is similarly overtwisted but with zero extension. For negative (left-handed) twisting, a highly extended and undertwisted DNA state (S-DNA) occurs, plus an additional undertwisted state with extension only slightly greater than that of B-DNA (“Z”-DNA). All of our results are also consistent with other experiments of Allemand *et al.* [20] which focused on transitions between B, P, and sc-P states.

The physical picture of simple structural transitions between these five states, driven by forces and torques, is supported by the good global fit that we can make for a simple five-state model to the experimental force-extension curves. From our model we predict a force-torque “phase diagram” in which the five structural states occur, separated by first-order-like transition lines. Given a micromanipulation experiment which can directly measure torque (e.g., by angular fluctuations of one end of the molecule), this phase diagram might be experimentally verified. All existing experimental data taken to date on dsDNA structural transitions have been done in the ensemble of fixed linkage number, and an outstanding experimental problem is how to directly measure the torque applied in those experiments.

### B. “Z”-DNA state and DNA strand separation

An important result of our analysis is that we need two undertwisted states in order to produce the two-plateau struc-



ture of the force-distance curves obtained for underwound DNA, namely, S-DNA and “Z”-DNA. The latter state is only 10% longer than the B-DNA double helix, but our best fit occurs when its helicity is roughly the reverse of that of B-DNA, i.e., a left-handed double helix with  $\approx 12$  bp per helix repeat. This state is distinct from S-DNA (S-DNA is about 70% longer than B-DNA and has a right-handed helix with 38 bp repeat). We use the name “Z”-DNA in imitation of the name given to the left-handed structure taken by some DNA sequences with similar length and helicity [27]. We stress that our ‘Z’-DNA occurs for undertwisted lambda-DNA, and is not stable at zero applied torque. Our “Z”-DNA is not obviously related to true Z-DNA.

It is possible that the torque-induced “Z”-DNA is to some degree strand-separated DNA [28]. However, this is difficult to determine from the current data since the micro-manipulation experiments done to date do not directly probe details of DNA structure. We did try to fit the experiments with  $\sigma = -1$ , which corresponds to parallel separated strands. Our model indicates that this cannot provide a good fit to the experimental plateau, and we conclude that if the “Z”-DNA state is in fact strand separated, those separated strands are then interwound to form a left-handed double helix with a 12 bp helix repeat and extension only slightly larger than that of B-DNA.

Finally, strand separation alone cannot explain the entire phase diagram since there are force-extension curves with

two plateaus. There must be some differences in secondary structure between adjacent distinct phases, with accompanying energetic differences, to account for the observed transitions. We certainly do not mean to rule out the possibility of some degree of disruption of double helix secondary structure in the four non-B states. For example, the P and sc-P states have been proposed to have no hydrogen bonding on the basis of experiments showing them to be chemically exposed [20], and this is certainly not in any contradiction with our model. In fact, disruption of base pairing is required to explain the very short (2.4 bp) helix repeat inferred for P-DNA from experimental data [20,13].

#### ACKNOWLEDGMENTS

We thank V. Croquette, J.-F. Allemand, T. Strick, and D. Bensimon for communication of their experimental data and for many helpful discussions. We are also indebted to I. Rouzina for helpful discussions. Work at UIC was supported by the Petroleum Research Foundation, the NSF through Grant. No. DMR-9734178, by the Research Corporation, by the Whitaker Foundation, and by the University of Illinois Foundation. Work at LDFC was supported by the Fondation pour la Recherche Medicale, the DRET-Ministere des Armees, the CNRS-MPCV, the Universite Louis Pasteur, and by NATO.

- 
- [1] J. Darnell, H. Lodish, and D. Baltimore, *Molecular Cell Biology* (Scientific American, New York, 1990), pp. 68–72.
- [2] K. J. Breslauer, R. Frank, H. Blocker, and L. A. Marky, *Proc. Natl. Acad. Sci. USA* **83**, 3746 (1986).
- [3] P. Cluzel, A. Lebrun, C. Heller, R. Lavery, J.-L. Viovy, D. Chatenay, and F. Caron, *Science* **271**, 792 (1996).
- [4] S. B. Smith, Y. Cui, and C. Bustamante, *Science* **271**, 795 (1996).
- [5] D. Bensimon, A. J. Simon, V. Croquette, and A. Bensimon, *Phys. Rev. Lett.* **74**, 4754 (1995).
- [6] H. Clausen-Schaumann, M. Rief, C. Tolksdorf, and H. E. Gaub, *Biophys. J.* **78**, 1997 (2000).
- [7] D. B. Nikolov, H. Chen, E. Halay, A. Usheva, K. Hisatake, D. K. Lee, R. G. Roeder, and S. K. Burley, *Nature (London)* **377**, 119 (1995).
- [8] K. Luger, A. W. Mader, R. K. Richmond, D. F. Sargent, and T. Richmond, *Nature (London)* **389**, 251 (1997).
- [9] A. Stasiak, E. di Capua, and Th. Koller, *J. Mol. Biol.* **151**, 557 (1981).
- [10] J.-F. Léger, J. Bourdieu, D. Chatenay, and J. F. Marko, *Proc. Natl. Acad. Sci. U.S.A.* **95**, 12 295 (1998).
- [11] T. R. Strick, J.-F. Allemand, D. Bensimon, A. Bensimon, and V. Croquette, *Science* **271**, 1835 (1996).
- [12] P. Cluzel, Ph.D. thesis, Universite Pierre et Marie Currie, Paris, 1996.
- [13] J. F. Léger, G. Romano, A. Sarkar, J. Robert, L. Bourdieu, D. Chatenay, and J. F. Marko, *Phys. Rev. Lett.* **83**, 1066 (1999).
- [14] J. F. Marko and E. D. Siggia, *Science* **265**, 506 (1994).
- [15] D. Moroz, and P. Nelson, *Proc. Natl. Acad. Sci. U.S.A.* **94**, 14 418 (1997).
- [16] C. Bouchiat, and M. Mezard, *Phys. Rev. Lett.* **80**, 1556 (1998).
- [17] A. V. Vologodskii, and J. F. Marko, *Biophys. J.* **73**, 123 (1997).
- [18] T. Strick, V. Croquette, and D. Bensimon, *Proc. Natl. Acad. Sci. U.S.A.* **95**, 10 579 (1998).
- [19] S. Cocco and R. Monasson, *Phys. Rev. Lett.* **83**, 5178 (1999).
- [20] J. F. Allemand, D. Bensimon, R. Lavery, and V. Croquette, *Proc. Natl. Acad. Sci. U.S.A.* **95**, 14 152 (1998).
- [21] S. B. Smith, L. Finzi, and C. Bustamante, *Science* **258**, 1122 (1992).
- [22] T. T. Perkins, S. R. Quake, D. E. Smith, and S. Chu, *Science* **264**, 822 (1994).
- [23] T. T. Perkins, D. E. Smith, R. G. Larson, and S. Chu, *Science* **268**, 83 (1995).
- [24] C. Bustamante, J. F. Marko, S. B. Smith, and E. D. Siggia, *Science* **265**, 1599 (1994).
- [25] A. Vologodskii, *Macromolecules* **27**, 5623 (1994).
- [26] A. Lebrun and R. Lavery, *Nucl. Acid Res.* **24**, 2260 (1996).
- [27] A. Herbert and A. Rich, *J. Biol. Chem.* **271**, 11 595 (1996).
- [28] I. Rouzina and V. Bloomfeld, *Biophys. J.* **80**, 882 (2001).
- [29] F. B. Fuller, *Proc. Natl. Acad. Sci. U.S.A.* **68**, 815 (1971).
- [30] N. R. Cozzarelli, T. C. Boles, and J. White, in *DNA Topology and its Biological Effects*, edited by N. R. Cozzarelli and J. C. Wang (Cold Spring Harbor Laboratory, Cold Spring Harbor, NY, 1990), Chap. 4.

- [31] S. B. Smith, Y. Cui, A. C. Hausrath, and C. Bustamante, *Biophys. J.* **68**, A250 (1995).
- [32] J. F. Marko, *Phys. Rev. E* **57**, 2134 (1998).
- [33] A. V. Vologodskii, *Topology and Physics of Circular DNA* (CRC Press, Boca Raton, FL, 1992).
- [34] T. R. Strick, D. Bensimon, and V. Croquette, in *Structural Biology and Functional Genomics*, edited by E. M. Bradbury and S. Pongor, NATO Science Series 3 (Kluwer Academic Publishers, Boston, 1999).